^{18}F-PI-2620 Tau PET Improves the Imaging Diagnosis of Progressive Supranuclear Palsy

Konstantin Messerschmidt*[1], Henryk Barthel*[1], Matthias Brendel*[2–4], Cordula Scherlach[5], Karl-Titus Hoffmann[5], Boris-Stephan Rauchmann[6], Michael Rullmann[1], Kenneth Marek[7], Victor L. Villemagne[8], Jost-Julian Rumpf[9], Dorothee Saur[9], Matthias L. Schroeter[10], Andreas Schildan[1], Marianne Patt[1], Leonie Beyer[2], Mengmeng Song[2], Carla Palleis[11], Sabrina Katzdobler[11], Urban M. Fietzek[11], Gesine Respondek[12], Maximilian Scheifele[2], Alexander Nitschmann[2], Christian Zach[2], Olivier Barret[7], Jennifer Madonia[7], David Russell[7], Andrew W. Stephens[13], Norman Koglin[13], Sigrun Roeber[14], Jochen Herms[14], Kai Bötzel[11], Peter Bartenstein[2], Johannes Levin[3,4,11], John P. Seibyl[7], Günter Höglinger[3,4,12], Joseph Classen[9], and Osama Sabri[1] for the German Imaging Initiative for Tauopathies (GII4T)

[1]Department of Nuclear Medicine, Leipzig University Medical Center, Leipzig, Germany; [2]Department of Nuclear Medicine, University Hospital of Munich, LMU Munich, Munich, Germany; [3]German Center for Neurodegenerative Diseases, Site Munich, Bonn, Germany; [4]Munich Cluster for Systems Neurology, Munich, Germany; [5]Department of Neuroradiology, Leipzig University Medical Center, Leipzig, Germany; [6]Department of Radiology, University Hospital of Munich, LMU Munich, Munich, Germany; [7]InviCRO LLC, Boston, Massachusetts; [8]Department of Psychiatry, University of Pittsburgh, Pittsburgh, Pennsylvania; [9]Department of Neurology, Leipzig University Medical Center, Leipzig, Germany; [10]Clinic for Cognitive Neurology, Leipzig University Medical Center, Leipzig, Germany; [11]Department of Neurology, University Hospital of Munich, LMU Munich, Munich, Germany; [12]Department of Neurology, Hannover Medical School, Hannover, Germany; [13]Life Molecular Imaging GmbH, Berlin, Germany; and [14]Center for Neuropathology and Prion Research, University Hospital of Munich, LMU Munich, Munich, Germany

Progressive supranuclear palsy (PSP) is a 4-repeat tauopathy movement disorder that can be imaged by the ^{18}F-labeled tau PET tracer 2-(2-([^{18}F]fluoro)pyridin-4-yl)-9H-pyrrolo[2,3-b:4,5-c']dipyridine (^{18}F-PI-2620). The in vivo diagnosis is currently established on clinical grounds and supported by midbrain atrophy estimation in structural MRI. Here, we investigate whether ^{18}F-PI-2620 tau PET has the potential to improve the imaging diagnosis of PSP. **Methods:** In this multicenter observational study, dynamic (0–60 min after injection) ^{18}F-PI-2620 PET and structural MRI data for 36 patients with PSP, 22 with PSP–Richardson syndrome, and 14 with a clinical phenotype other than Richardson syndrome (i.e., variant PSP) were analyzed along with data for 10 age-matched healthy controls (HCs). The PET data underwent kinetic modeling, which resulted in distribution volume ratio (DVR) images. These and the MR images were visually assessed by 3 masked experts for typical PSP signs. Furthermore, established midbrain atrophy parameters were measured in structural MR images, and regional DVRs were measured in typical tau-in-PSP target regions in the PET data. **Results:** Visual assessments discriminated PSP patients and HCs with an accuracy of 63% for MRI and 80% for the combination of MRI and ^{18}F-PI-2620 PET. As compared with patients of the PSP–Richardson syndrome subgroup, those of the variant PSP subgroup profited more in terms of sensitivity from the addition of the visual ^{18}F-PI-2620 PET to the visual MRI information (35% vs. 22%). In quantitative image evaluation, midbrain-to-pons area ratio and globus pallidus DVRs discriminated best between the PSP patients and HCs, with sensitivities and specificities of 83% and 90%, respectively, for MRI and 94% and 100%, respectively, for the combination of MRI and ^{18}F-PI-2620 PET. The gain of sensitivity by adding ^{18}F-PI-2620 PET to MRI data was more marked in clinically less affected patients than in more affected patients (37% vs. 19% for visual, and 16% vs. 12% for quantitative image evaluation). **Conclusion:** These results provide evidence for an improved imaging-based PSP diagnosis by adding ^{18}F-PI-2620 tau PET to structural MRI. This approach seems to be particularly promising at earlier disease stages and could be of value both for improving early clinical PSP diagnosis and for enriching PSP cohorts for trials of disease-modifying drugs.

Key Words: ^{18}F-PI-2620; 4R-tauopathy; progressive supranuclear palsy; tau PET; midbrain atrophy

The clinicopathologic syndrome of progressive supranuclear palsy (PSP), which was initially described by Steele et al. (1), is a 4-repeat tauopathy movement disorder and is counted among the atypical parkinsonian disorders (2,3). Symptoms include ocular motor abnormalities, postural instability, akinesia, and cognitive impairment, among others. The disease leads to death within a mean of 6–8 y after symptom onset (4,5). Age-adjusted prevalence was recently estimated in Europe at 8.8 per 100,000 patients and in Japan at 17.3 per 100,000 patients (6,7). Compared with postmortem histopathology as the diagnostic gold standard, the diagnostic accuracy of clinical assessment is limited by overlap of symptoms with those of other neurodegenerative diseases such as Parkinson disease, corticobasal degeneration, and frontotemporal dementia (8–10). As a consequence, according to current PSP diagnostic criteria, clinical testing can be supplemented by imaging-based biomarkers. These include structural MRI, ^{18}F-FDG PET, and dopamine D_2/D_3 receptor imaging (10). The typical PSP signs in structural MRI are related to midbrain atrophy and include the hummingbird sign, the morning glory sign, and the Mickey Mouse sign (11–14). MRI morphometry of the midbrain and related structures also serves this purpose (15–19). Midbrain atrophy in PSP

is believed to be a late-stage consequence of preceding molecular processes. Therefore, molecular biomarkers of tau pathology are expected to be more sensitive than structural MRI in supporting the PSP diagnosis. However, molecular biomarkers of tau pathology in PSP are still missing (20). We recently showed that 2-(2-([18F]fluoro)-pyridin-4-yl)-9H-pyrrolo[2,3-b:4,5-c′]dipyridine (18F-PI-2620), a 18F-labeled PET tracer with high affinity to aggregated tau, is able to provide valuable diagnostic information on PSP patients (21). Thus, it was the aim of this follow-up evaluation to investigate how the diagnostic potential of 18F-PI-2620 PET relates to that of midbrain MRI, the current in vivo imaging standard in PSP.

MATERIALS AND METHODS

This study was an add-on project of the multicenter observational study of the German Imaging Initiative for Tauopathies investigating the potential of 18F-PI-2620 tau PET imaging in PSP, the main results of which were recently published elsewhere (21). Patients with probable or possible PSP according to current diagnosis criteria (10) were included, together with healthy controls (HCs). The data analysis was approved by the local Ethics Committee of the Ludwig Maximilian University of Munich (approvals 17-569 and 19-022). All subjects provided written informed consent before participating in the study. The study was registered at the German Clinical Trials Register (DRKS00016920).

The brain MR images were acquired either on a 3-T hybrid PET/MRI system (Biograph mMR [Siemens], $n = 16$) or on a stand-alone 1.5- or 3-T MRI system ($n = 30$). Standard structural T1-weighted MR images were analyzed either as single 3-dimensional or multiple sequences in different planes. These included 3-dimensional magnetization-prepared rapid gradient-echo sequences, 3-dimensional magnetization-prepared 2 rapid-acquisition gradient-echo sequences, 3-dimensional fast spoiled gradient-echo sequences, ultrashort-echo-time enhanced sequences, and turbo field-echo sequences. The MR images were visually evaluated by 3 experienced neuroradiologists. They were masked to the subject subgroup allocation and the other reader scores. The readers scored for the presence or absence of the established midbrain atrophy signs: the hummingbird sign, pointing to rostral midbrain atrophy in midsagittal MR images; the Mickey Mouse sign, describing the reduced midbrain diameter with relative preservation of tectum and cerebral peduncles in axial MR images; and the morning glory sign, pointing to the concavity of the lateral margin of the tegmentum of the midbrain, also in axial MR images (11–13). For that purpose, the individual MR images were presented to the readers as NIfTI files using the Papaya online medical research image viewer (https://github.com/rii-mango/Papaya). They were judged as positive for PSP if at least 1 of the above signs was positive. To allow determining the intrareader reliability, the MR images of a randomly chosen and remixed subset of 8 PSP patients and HCs (representing ∼20% [8/46] of the study cohort) were reevaluated 3 mo after the initial read. In addition to the visual analysis, midbrain atrophy was determined quantitatively in the MR images by measuring the following established parameters in the Hybrid Viewer PDR (version 5.1.0) software on an image analysis workstation (Hermes Medical Solutions): midbrain diameter, midbrain area, midbrain-to-pons area ratio, and MR parkinsonism index ([pons-to-midbrain area ratio] × [middle cerebellar peduncle–to–superior cerebellar peduncle diameter ratio]) (22).

18F-PI-2620 tau PET image acquisition and processing were described in detail elsewhere (21). In short, PET imaging was performed dynamically 0–60 min after injection of about 300 MBq on hybrid PET/MRI or PET/CT systems. Voxel-based distribution volume ratios (DVRs) were determined in PMOD (version 3.9; PMOD Inc.) using the multilinear reference tissue model 2, with the cerebellum (excluding the dentate nucleus and the central cerebellar white matter, as well as the superior and the posterior cerebellar layers) as the reference region (23). As with the MRI data, the resulting parametric DVR maps were analyzed visually and quantitatively. Using a previously described scoring system (21), visual evaluation was performed by 3 experienced nuclear physicians who were masked to the subject subgroup allocation and the other reader scores. The presence or absence of a PSP-typical binding pattern involving the putamen, the subthalamic nucleus, the globus pallidus, the substantia nigra, and the dentate nucleus was evaluated, leading to a binary (tau-positive or -negative) categorization of each individual PET scan (21). Three months after the initial read, we reevaluated the DVR images of the same randomly chosen and remixed subset of 8 PSP patients and HCs whose MR images were reevaluated. In addition to the visual PET evaluation, regional DVRs were obtained via volume-of-interest analysis for the same tau-in-PSP target regions as analyzed visually (21).

Statistical testing was performed on SPSS (version 25.0; IBM). For the visual image analysis, interrater agreement was calculated using the Fleiss κ, and intrarater agreement was evaluated using the percentage of accordance. For the quantitative image data, receiver-operator-characteristic curves were analyzed. Spearman correlation coefficients were calculated between the demographic, clinical, and imaging parameters, determining false-discovery rates to correct for random associations. P values of less than 0.05 were considered significant.

RESULTS

Demographics

From the original study cohort (21), structural brain MRI within 6 mo of the 18F-PI-2620 tau PET imaging was available for 36 patients (71 ± 8 y old, 16 women) with probable or possible PSP and in 10 age-matched HCs (67 ± 7 y old, 8 women). For the PSP patients, disease duration, defined as the time between symptom onset and PET imaging, was 3.3 ± 2.6 y. PSP rating scores were 31 ± 13, and functional ability Schwab and England activities-of-daily-living scores were 60 ± 19. The PSP group consisted of 22 patients with PSP–Richardson syndrome (PSP-RS) and 14 patients with a clinical phenotype other than Richardson syndrome, that is, variant PSP (vPSP; PSP–corticobasal syndrome [$n = 7$], PSP-parkinsonism [$n = 3$], PSP-frontal [$n = 3$], and PSP-speech/language [$n = 1$]).

Visual Image Evaluation

The results of the visual MR image evaluation by the 3 masked neuroradiologists are given in Table 1. Although 100% (10/10) specificity in the discrimination between PSP patients and HCs was achieved, the sensitivity of the MRI majority read was 53% (19/36; accuracy, 63%). For interreader agreement, the Fleiss κ equaled 0.76 for the MRI read, whereas intrareader MRI agreement ranged from 88% to 100% (7/8–8/8). The results of the visual 18F-PI-2620 PET image evaluation by the 3 masked nuclear physicians are likewise given in Table 1. The 18F-PI-2620 PET majority read achieved a sensitivity of 75% (27/36) and a specificity of 80% (8/10; accuracy, 76%). For interreader agreement, the Fleiss κ equaled 0.59 for the 18F-PI-2620 PET read, whereas intrareader 18F-PI-2620 PET agreement again ranged from 88% to 100% (7/8–8/8). Figure 1 shows MRI and 18F-PI-2620 PET images of a typical PSP patient and a typical HC, illustrating that it was quite possible for the readers to spot the respective PSP signs on an individual level (individual 18F-PI-2620 PET and MRI images of each patient or HC). Of interest, combining the majority MRI and majority 18F-PI-2620 PET read results in such a way that at least 1 modality that was positive made the brain positive for PSP resulted in a sensitivity of 81% (29/36) and a specificity of 80% (8/10; accuracy, 80%; Table 1).

TABLE 1
Visual Image Data Evaluation

Parameter	Sensitivity	Specificity	Accuracy
MRI reader 1	61% (22/36)	100% (10/10)	70
MRI reader 2	47% (17/36)	100% (10/10)	59
MRI reader 3	56% (20/36)	100% (10/10)	65
MRI majority read	53% (19/36)	100% (10/10)	63
^{18}F-PI-2620 PET reader 1	86% (31/36)	40% (4/10)	76
^{18}F-PI-2620 PET reader 2	72% (26/36)	90% (9/10)	76
^{18}F-PI-2620 PET reader 3	69% (25/36)	90% (9/10)	74
^{18}F-PI-2620 PET majority read	75% (27/36)	80% (8/10)	76
^{18}F-PI-2620 PET + MRI	81% (29/36)	80% (8/10)	80

For combination of ^{18}F-PI-2620 PET and MRI, ≥ 1 abnormal parameter that was positive made brain positive for PSP.

Visual MRI analysis was less sensitive in the vPSP patients than in the PSP-RS patients, although the sensitivity of the visual ^{18}F-PI-2620 PET analysis did not differ between the 2 subgroups. Consequently, the vPSP patients profited more than the PSP-RS patients in terms of sensitivity from the addition of the visual ^{18}F-PI-2620 PET to the visual MRI information (35% vs. 22%; Supplemental Table 1; supplemental materials are available at http://jnm.snmjournals.org).

Quantitative Image Evaluation

The results of the receiver-operator-characteristic curve analyses for the different quantitative MRI and ^{18}F-PI-2620 PET parameters and the resulting diagnostic quality parameters in discriminating PSP patients from HCs are provided in Table 2. While, for the MRI parameters, the midbrain/pons area ratio was revealed to have the highest discriminative power, this was the case for the globus pallidus DVRs with respect to the ^{18}F-PI-2620 PET parameters. To investigate the main study question of whether the

FIGURE 1. Axial ^{18}F-PI-2620 tau PET and sagittal T1-weighted 3-dimensional magnetization-prepared 2 rapid-acquisition gradient-echo structural MR images of PSP patient and of HC. Pathologic ^{18}F-PI-2620 binding is seen in globus pallidus (white arrow), in striatum, and in subthalamic nucleus of PSP patient. Hummingbird sign (yellow arrow) due to atrophy of rostral midbrain is seen in structural MR image of PSP patient. No pathologic ^{18}F-PI-2620 binding is present in HC, and midbrain appears normal.

^{18}F-PI-2620 PET information can enhance the ability of in vivo imaging to diagnose PSP, we combined the above 2 parameters toward a tau-PET/MRI-in-PSP index (^{18}F-PI-2620 PET globus pallidus DVR × MRI midbrain-to-pons area ratio^{-1}). Of interest, this tau-PET/MRI-in-PSP index achieved a higher Cohen d effect (2.06; Fig. 2) and a higher area under the receiver-operator-characteristic curve (0.98; Fig. 3) than did the MRI midbrain-to-pons area ratio alone (1.96 and 0.93). The sensitivity and specificity of the tau-PET/MRI-in-PSP index in discriminating PSP patients from HCs were 94% and 100% (34/36 and 10/10; accuracy, 96%), whereas those of the MRI midbrain-to-pons area ratio were 83% and 90% (30/36 and 9/10; accuracy, 85%). No differences (after correction for multiple comparisons) were found for the MRI and ^{18}F-PI-2620 PET parameters between the PSP-RS and vPSP subgroups. In the vPSP subgroup, quantitative ^{18}F-PI-2620 PET data analysis was less sensitive than in the PSP-RS subgroup. Apart from that, the quantitative image analysis results did not relevantly differ between the 2 subgroups (Supplemental Table 2).

Association Between Imaging and Demographic/Clinical Data

The associations between the demographic/clinical, quantitative MRI, and quantitative ^{18}F-PI-2620 PET parameters are provided in Figure 4. We checked for correlations of the PSP rating scale and Schwab and England activities-of-daily-living scores with different MRI parameters and correlations of the PSP rating scores with the tau-PET/MRI-in-PSP indices. No correlation with any imaging parameter was found for disease duration. There were several intercorrelations among the different MRI, ^{18}F-PI-2620 PET, and ^{18}F-PI-2620 PET + MRI (tau-PET/MRI-in-PSP index) parameters (Fig. 4). The respective results for the 2 PSP subgroups are provided in Supplemental Figure 1. Interestingly, several of these intercorrelations between different imaging readouts were not observed when investigating the vPSP subgroup (Supplemental Fig. 1).

We were also interested in whether and to what degree the diagnostic potentials of MRI and ^{18}F-PI-2620 PET depend on disease stage. To investigate this dependence, we built 2 PSP patient subgroups according to their PSP rating scores applying a mean value-split—that is, applying the mean value of our PSP patient cohort of 31 as a separation threshold. Here, the gain in sensitivity by adding ^{18}F-PI-2620 PET to MRI was more pronounced in the subgroup with a PSP rating score of less than 31 ($n = 19$; 53% vPSP) than in the subgroup with a PSP rating score of 31 or higher
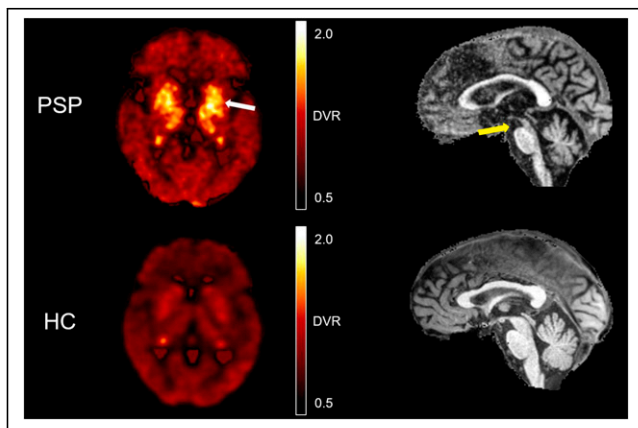
TABLE 2
Quantitative Image Data Analysis

Parameter	PSP patients*	HCs*	P (t test)	Cohen d	AUC$_{ROC}$
MRI					
MB diameter (mm)	15.2 ± 1.9	16.4 ± 1.4	NS	0.74	0.70
MB area (mm^2)	108.8 ± 32.5	165.5 ± 23.9	<0.0001	1.99	0.92
MB-to-pons area ratio	0.19 ± 0.04	0.28 ± 0.05	<0.0001	1.96	0.93
MRPI	15.6 ± 5.7	9.2 ± 1.5	0.001	1.54	0.92
^{18}F-PI-2620 PET					
GP DVR	1.16 ± 0.11	0.99 ± 0.06	<0.0001	1.91	0.91
PUT DVR	1.19 ± 0.11	1.02 ± 0.06	<0.0001	1.89	0.90
STN DVR	1.20 ± 0.09	1.04 ± 0.09	<0.0001	1.73	0.91
SN DVR	1.17 ± 0.10	1.10 ± 0.07	NS	0.78	0.71
DN DVR	1.13 ± 0.05	1.06 ± 0.04	0.0001	1.67	0.88
Tau-PET/MRI-in-PSP index	6.29 ± 1.77	3.57 ± 0.58	<0.0001	2.06	0.98

*Values are mean ± SD.

AUC$_{ROC}$ = area under receiver-operator-characteristic curve; MB = midbrain; MRPI = MR parkinsonism index; GP = globus pallidus; PUT = putamen; STN = subthalamic nucleus; SN = substantia nigra; NS = not statistically significant; DN = dentate nucleus.

(n = 16; 25% vPSP). Furthermore, the subgroup with a PSP rating score of less than 31 had a more pronounced gain in sensitivity for the visual analysis than for the quantitative image analysis (Fig. 5).

DISCUSSION

In this study, we found that ^{18}F-PI-2620 tau PET improves the imaging-based diagnosis of PSP. Specifically, we focused on answering the question of whether ^{18}F-PI-2620 tau PET has an additional value in terms of imaging-based PSP diagnosis when combined with structural MRI information. The combination of both imaging readouts led to higher sensitivity in discriminating between PSP patients and HCs for both visual and quantitative assessment, and to a higher specificity for the quantitative image analysis. Of interest, the gain in sensitivity by adding ^{18}F-PI-2620 PET to MRI was more marked in clinically less affected patients than in more affected patients.

Currently, structural MRI represents the best-validated PSP biomarker (24). Our results for visual evaluation of structural MRI for discriminating between PSP patients and HCs (sensitivity, 53% [19/36]; specificity, 100% [10/10]) are comparable to those of previous investigations, which showed sensitivities in the range of 48%–85% combined with high specificities of 80%–100%
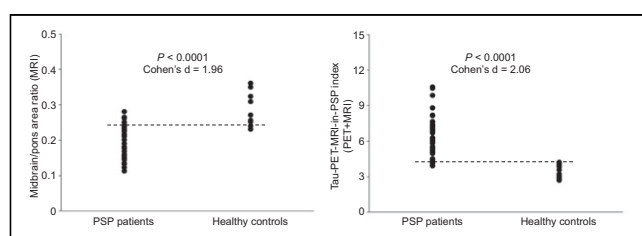
(13,25,26). Markedly higher diagnostic accuracy was seen only in those structural MRI studies with smaller sample sizes, that is, with fewer than 10 patients each (11,27). According to our receiver-operator-characteristic curve analysis, the midbrain-to-pons area ratio was the best structural MRI discriminator between PSP patients and HCs. This finding is likewise in accordance with previously reported findings (15,18,28–36).

To our knowledge, this study was the first that investigated the diagnostic potential of a second-generation tau PET tracer when
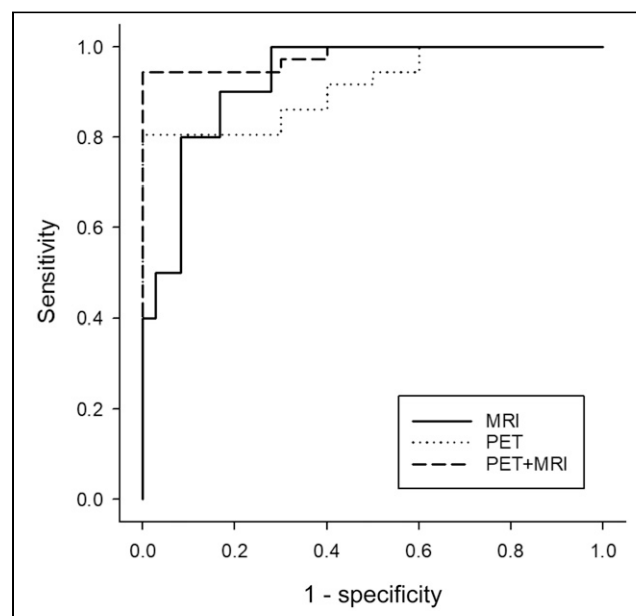

FIGURE 2. Scatterplots for MRI (midbrain-to-pons area ratio) parameter that discriminated best between patients with PSP and HCs, and for tau-PET/MRI-in-PSP index.

FIGURE 3. Receiver-operator-characteristic curves for MRI (midbrain-to-pons area ratio) and ^{18}F-PI-2620 PET (globus pallidus DVR) parameters that discriminated best for each technique between patients with PSP and HCs, and for tau-PET/MRI-in-PSP index.
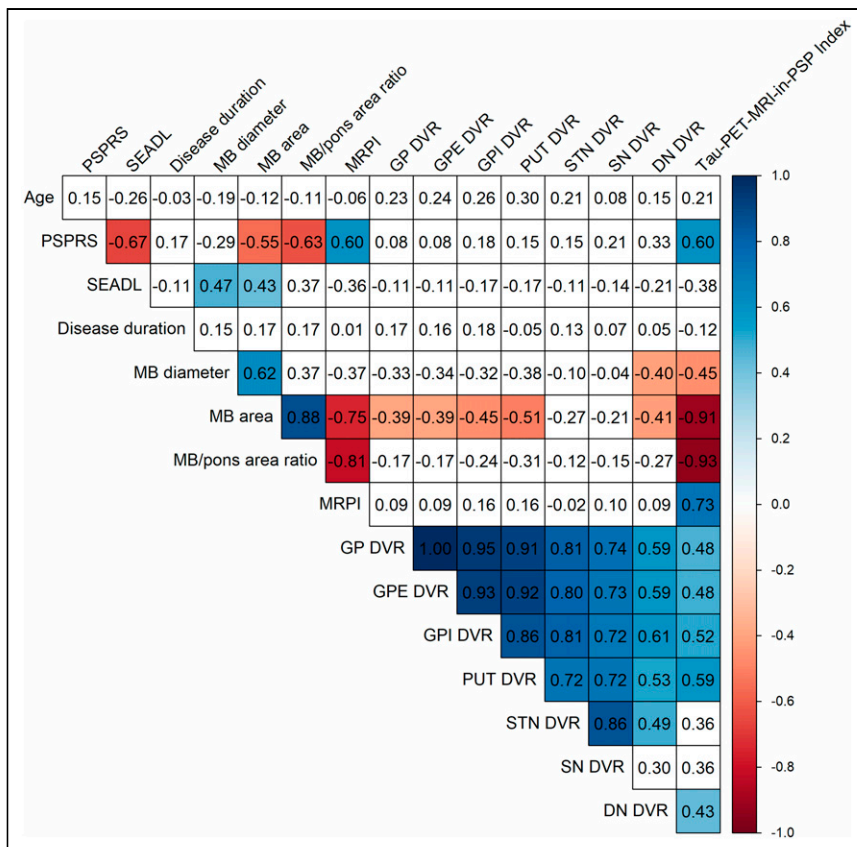
FIGURE 4. Association between age, disease duration, disease severity, structural MRI, and ^{18}F-PI-2620 tau PET parameters in patients with PSP. Values are correlation coefficients. Significant correlations ($P < 0.05$ after false-discovery-rate correction) are colorized according to scale on right. DN = dentate nucleus; GP = globus pallidus; GPE = globus pallidus externus; GPI = globus pallidus internus; MB = midbrain; MRPI = MR parkinsonism index; PSPRS = PSP rating scale; PUT = putamen; SEADL = Schwab and England activities-of-daily-living scale; SN = substantia nigra; STN = subthalamic nucleus.

added to structural MRI to diagnose PSP. First-generation tau PET tracers such as ^{18}F-AV-1451 and ^{18}F-THK5351 were reported to be capable of differentiating PSP patients from HCs (37–42). A drawback to most of these tracers is that relevant portions of them do not bind to aggregated tau (off-target binding, such as to monoamine oxidase-B) (42). As such, the effect sizes achieved with these tracers in PSP-versus-HC discrimination are believed to be related to a combined tau pathology and neuroinflammation effect. It is desirable to obtain a specific tau readout by PET imaging, especially in applications for differential diagnosis, disease progression, and therapy monitoring. ^{18}F-PI-2620, the PET tracer used in this project, has high in vitro affinity to recombinant 4R tau fibrils and PSP brain homogenate, as well as absence of off-target binding to monoamine oxidases (43). As we have also recently shown, ^{18}F-PI-2620 PET is able to discriminate between PSP patients and HCs in vivo with high accuracy. The sensitivity in our previous study was higher in the PSP-RS subgroup than in vPSP patients. We were able to replicate these finding in our currently investigated subpopulation of subjects for whom structural brain MRI data were available. The elevated ^{18}F-PI-2620 binding in the globus pallidus of the PSP patients as compared with the HCs is in line with earlier studies with the first-generation tau PET tracers ^{18}F-AV-1451 and ^{18}F-THK5351 (21,37,38,44,45). Other recent studies evaluated the second-generation tau PET tracer

^{18}F-PM-PBB3 and reported a sensitivity of 85%–94% and a specificity of 92%–100% in discriminating between PSP patients and HCs for SUVRs in typical tau-in-PSP regions (46,47). Altogether, our results and those of the recent ^{18}F-PM-PBB3 study underline the great potential of tau PET imaging as a biomarker of PSP.

In our study cohort, several quantitative MRI parameters and the newly proposed tau-PET/MRI-in-PSP index, but not the solely quantitative ^{18}F-PI-2620 PET parameters, correlated with the severity of clinical symptoms. This constellation differed between PSP-RS and vPSP patients. However, our results are in line with those of a longitudinal head-to-head comparison in PSP patients between MRI and ^{18}F-AV-1451 PET revealing progressing midbrain atrophy but no significant correlations between ^{18}F-AV-1451 binding and changes in the PSP rating scores during a 12-mo period (48). Other previous tau PET studies using ^{18}F-PI-2620, ^{18}F-AV-145, ^{18}F-THK5351, and ^{18}F-PM-PBB3 investigating this feature showed inconsistent results (21,37,38,45,47,49). Moreover, such data on PSP showing tau deposition as a function of disease duration are still limited today (50). Therefore, longitudinal studies investigating the value of ^{18}F-PI-2620 PET as an adjunct to structural MRI, potentially also using the newly proposed tau-PET/MRI-in-PSP index, are needed as a disease progression biomarker in PSP and as a way to monitor antitau treatments. Importantly, the potential of ^{18}F-PI-2620 PET to improve early PSP diagnosis, as implicated by the present study, deserves further clinical testing.

We found that the sensitivity gain by adding ^{18}F-PI-2620 PET to MRI was pronounced in clinically less affected—as compared with more affected—patients. This effect was evident both for visual and for quantitative image evaluation. This result fits the widely accepted disease model that PSP is a primary tauopathy, with atrophy being a consequence of tau pathology (8). Thus, ^{18}F-PI-2620 PET seems to have particular value as a biomarker for early PSP detection, that is, in PSP patients for whom neurodegeneration has not yet progressed enough to be visible as macroscopic atrophy. Thus, assuming replication of these results in prospective studies, ^{18}F-PI-2620 PET appears to be a promising candidate, particularly for improved screening of PSP patients for drug-testing trials.

As a study limitation, we cannot exclude that, because of the observational character of this study, the results of the MRI examination influenced patient inclusion. MRI is regularly used in such patients when the diagnosis is initially established, primarily to exclude other pathologies, such as vascular lesions, tumors, or inflammatory disorders. It cannot be excluded that, at least in several patients, the presence of midbrain atrophy was likewise evaluated on previous MR images and was considered supporting evidence when establishing the clinical diagnosis. This possibility would introduce a bias in favor of the MRI accuracy in our study. Only a prospective clinical study based solely on clinical criteria
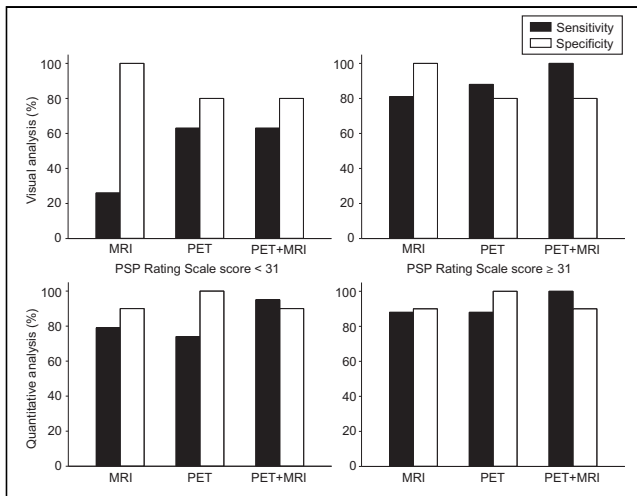
FIGURE 5. Sensitivities and specificities for discrimination between PSP patients and HCs by means of MRI, ^{18}F-PI-2620 PET, and combination of both techniques for 2 disease-severity subgroups of PSP patients separated by PSP rating score of 31 (mean value of entire PSP population). Results are shown for visual and quantitative image analyses. For combination of both modalities (^{18}F-PI-2620 PET + MRI), ≥1 abnormal parameter that was positive made brain positive for PSP. Gain of sensitivity was most pronounced by addition of ^{18}F-PI-2620 PET to MRI information for subgroup with visual image analysis of PSP rating score of <31.

for PSP patients or—ideally—a histopathology confirmation study would be able to provide bias-free evidence. Another limitation is the limited interrater reproducibility of the ^{18}F-PI-2620 PET read and the use of a majority decision (aggregating the results of the 3 readers) in the MRI and PET reads. Both points impact the prediction of how a ^{18}F-PI-2620 PET read will perform in future clinical praxis in which it is likely that there would be only 1 reader. Optimized reader training, which our group is already developing, seems needed to solve this problem and to tackle the current (less pronounced than the win in sensitivity) loss of specificity by the addition of the visual PET to the visual MRI information.

CONCLUSION

Our study demonstrated that, when added to structural MRI, ^{18}F-PI-2620 PET has the potential to improve the imaging-based diagnosis of PSP, especially at early disease. This finding supports the notion that ^{18}F-PI-2620 tau PET represents a valuable biomarker in PSP, both for clinical applications and for drug testing.

DISCLOSURE

<div style="border:1px solid black; padding:4px; display:inline-block;">KEY POINTS</div>

QUESTION: Does ^{18}F-PI-2620 tau PET improve the imaging diagnosis of PSP, especially when compared with structural MRI information?

PERTINENT FINDINGS: The combination of ^{18}F-PI-2620 tau PET with structural MRI led to higher sensitivity in discriminating between PSP patients and HCs for both visual and quantitative assessment, as well as leading to a higher specificity for quantitative image analysis. The gain in sensitivity by adding ^{18}F-PI-2620 PET to MRI was more marked in clinically less affected patients than in more affected patients.

IMPLICATIONS FOR PATIENT CARE: ^{18}F-PI-2620 PET appears to be a valuable biomarker in PSP and could be of value both for improving early clinical PSP diagnosis and for enriching PSP cohorts for trials of disease-modifying drugs.

REFERENCES

1. Steele JC, Richardson JC, Olszewski J. Progressive supranuclear palsy: a heterogeneous degeneration involving the brain stem, basal ganglia and cerebellum with vertical gaze and pseudobulbar palsy, nuchal dystonia and dementia. *Arch Neurol.* 1964;10:333–359.

2. Dickson DW, Ahmed Z, Algom AA, Tsuboi Y, Josephs KA. Neuropathology of variants of progressive supranuclear palsy. *Curr Opin Neurol.* 2010;23:394–400.

3. Rösler TW, Tayaranian Marvian A, Brendel M, et al. Four-repeat tauopathies. *Prog Neurobiol.* 2019;180:101644.

4. Litvan I, Mangone CA, McKee A, et al. Natural history of progressive supranuclear palsy (Steele-Richardson-Olszewski syndrome) and clinical predictors of survival: a clinicopathological study. *J Neurol Neurosurg Psychiatry.* 1996;60:615–620.

5. Respondek G, Stamelou M, Kurz C, et al.; Movement Disorder Society-endorsed PSP Study Group. The phenotypic spectrum of progressive supranuclear palsy: a retrospective multicenter study of 100 definite cases. *Mov Disord.* 2014;29:1758–1766.

6. Fleury V, Brindel P, Nicastro N, Burkhard PR. Descriptive epidemiology of parkinsonism in the Canton of Geneva, Switzerland. *Parkinsonism Relat Disord.* 2018;54:30–39.

7. Takigawa H, Kitayama M, Wada-Isoe K, Kowa H, Nakashima K. Prevalence of progressive supranuclear palsy in Yonago: change throughout a decade. *Brain Behav.* 2016;6:e00557.

8. Williams DR, Lees AJ. Progressive supranuclear palsy: clinicopathological concepts and diagnostic challenges. *Lancet Neurol.* 2009;8:270–279.

9. Boxer AL, Yu JT, Golbe LI, Litvan I, Lang AE, Höglinger GU. Advances in progressive supranuclear palsy: new diagnostic criteria, biomarkers, and therapeutic approaches. *Lancet Neurol.* 2017;16:552–563.

10. Höglinger GU, Respondek G, Stamelou M, et al.; Movement Disorder Society-endorsed PSP Study Group. Clinical diagnosis of progressive supranuclear palsy: the Movement Disorder Society criteria. *Mov Disord.* 2017;32:853–864.

11. Kato N, Arai K, Hattori T. Study of the rostral midbrain atrophy in progressive supranuclear palsy. *J Neurol Sci.* 2003;210:57–60.

12. Adachi M, Kawanami T, Ohshima H, Sugai Y, Hosoya T. Morning glory sign: a particular MR finding in progressive supranuclear palsy. *Magn Reson Med Sci.* 2004;3:125–132.

13. Massey LA, Micallef C, Paviour DC, et al. Conventional magnetic resonance imaging in confirmed progressive supranuclear palsy and multiple system atrophy. *Mov Disord.* 2012;27:1754–1762.

14. Stamelou M, Knake S, Oertel WH, Höglinger GU. Magnetic resonance imaging in progressive supranuclear palsy. *J Neurol.* 2011;258:549–558.

15. Massey LA, Jäger HR, Paviour DC, et al. The midbrain to pons ratio: a simple and specific MRI sign of progressive supranuclear palsy. *Neurology.* 2013;80:1856–1861.

16. Quattrone A, Nicoletti G, Messina D, et al. MR imaging index for differentiation of progressive supranuclear palsy from Parkinson disease and the Parkinson variant of multiple system atrophy. *Radiology.* 2008;246:214–221.

17. Nigro S, Arabia G, Antonini A, et al. Magnetic Resonance Parkinsonism Index: diagnostic accuracy of a fully automated algorithm in comparison with the manual measurement in a large Italian multicentre study in patients with progressive supranuclear palsy. *Eur Radiol.* 2017;27:2665–2675.

18. Hussl A, Mahlknecht P, Scherfler C, et al. Diagnostic accuracy of the magnetic resonance Parkinsonism index and the midbrain-to-pontine area ratio to differentiate progressive supranuclear palsy from Parkinson's disease and the Parkinson variant of multiple system atrophy. *Mov Disord.* 2010;25:2444–2449.

19. Morelli M, Arabia G, Novellino F, et al. MRI measurements predict PSP in unclassifiable parkinsonisms: a cohort study. *Neurology.* 2011;77:1042–1047.

20. van Eimeren T, Antonini A, Berg D, et al. Neuroimaging biomarkers for clinical trials in atypical parkinsonian disorders: proposal for a Neuroimaging Biomarker Utility System. *Alzheimers Dement (Amst).* 2019;11:301–309.

21. Brendel M, Barthel H, van Eimeren T, et al. Assessment of ^{18}F-PI-2620 as a biomarker in progressive supranuclear palsy. *JAMA Neurol.* 2020;77:1408–1419.

22. Möller L, Kassubek J, Südmeyer M, et al. Manual MRI morphometry in Parkinsonian syndromes. *Mov Disord.* 2017;32:778–782.

23. Ichise M, Liow JS, Lu JQ, et al. Linearized reference tissue parametric imaging methods: application to [11C]DASB positron emission tomography studies of the serotonin transporter in human brain. *J Cereb Blood Flow Metab.* 2003;23:1096–1112.

24. Whitwell JL, Höglinger GU, Antonini A, et al.; Movement Disorder Society-endorsed PSP Study Group. Radiological biomarkers for diagnosis in PSP: where are we and where do we need to be? *Mov Disord.* 2017;32:955–971.

25. Kim YE, Kang SY, Ma HI, Ju YS, Kim YJ. A visual rating scale for the hummingbird sign with adjustable diagnostic validity. *J Parkinsons Dis.* 2015;5:605–612.

26. Wadia PM, Howard P, Ribeirro MQ, et al. The value of GRE, ADC and routine MRI in distinguishing Parkinsonian disorders. *Can J Neurol Sci.* 2013;40:389–402.

27. Meijer FJ, van Rumund A, Tuladhar AM, et al. Conventional 3T brain MRI and diffusion tensor imaging in the diagnostic workup of early stage parkinsonism. *Neuroradiology.* 2015;57:655–669.

28. Oba H, Yagishita A, Terada H, et al. New and reliable MRI diagnosis for progressive supranuclear palsy. *Neurology.* 2005;64:2050–2055.

29. Cosottini M, Ceravolo R, Faggioni L, et al. Assessment of midbrain atrophy in patients with progressive supranuclear palsy with routine magnetic resonance imaging. *Acta Neurol Scand.* 2007;116:37–42.

30. Kaasinen V, Kangassalo N, Gardberg M, et al. Midbrain-to-pons ratio in autopsy-confirmed progressive supranuclear palsy: replication in an independent cohort. *Neurol Sci.* 2015;36:1251–1253.

31. Kim YH, Ma HI, Kim YJ. Utility of the midbrain tegmentum diameter in the differential diagnosis of progressive supranuclear palsy from idiopathic Parkinson's disease. *J Clin Neurol.* 2015;11:268–274.

32. Longoni G, Agosta F, Kostić VS, et al. MRI measurements of brainstem structures in patients with Richardson's syndrome, progressive supranuclear palsy-parkinsonism, and Parkinson's disease. *Mov Disord.* 2011;26:247–255.

33. Looi JC, Macfarlane MD, Walterfang M, et al. Morphometric analysis of subcortical structures in progressive supranuclear palsy: in vivo evidence of neostriatal and mesencephalic atrophy. *Psychiatry Res.* 2011;194:163–175.

34. Morelli M, Arabia G, Salsone M, et al. Accuracy of magnetic resonance parkinsonism index for differentiation of progressive supranuclear palsy from probable or possible Parkinson disease. *Mov Disord.* 2011;26:527–533.

35. Zanigni S, Calandra-Buonaura G, Manners DN, et al. Accuracy of MR markers for differentiating progressive supranuclear palsy from Parkinson's disease. *Neuroimage Clin.* 2016;11:736–742.

36. Albrecht F, Bisenius S, Neumann J, Whitwell J, Schroeter ML. Atrophy in midbrain & cerebral/cerebellar pedunculi is characteristic for progressive supranuclear palsy: a double-validation whole-brain meta-analysis. *Neuroimage Clin.* 2019;22:101722.

37. Schonhaut DR, McMillan CT, Spina S, et al. 18F-flortaucipir tau positron emission tomography distinguishes established progressive supranuclear palsy from controls and Parkinson disease: a multicenter study. *Ann Neurol.* 2017;82:622–634.

38. Brendel M, Schönecker S, Höglinger G, et al. [18F]-THK5351 PET correlates with topology and symptom severity in progressive supranuclear palsy. *Front Aging Neurosci.* 2018;9:440.

39. Passamonti L, Vázquez Rodríguez P, Hong YT, et al. 18F-AV-1451 positron emission tomography in Alzheimer's disease and progressive supranuclear palsy. *Brain.* 2017;140:781–791.

40. Marquié M, Verwer EE, Meltzer AC, et al. Lessons learned about [F-18]-AV-1451 off-target binding from an autopsy-confirmed Parkinson's case. *Acta Neuropathol Commun.* 2017;5:75.

41. Marquié M, Normandin MD, Meltzer AC, et al. Pathological correlations of [F-18]-AV-1451 imaging in non-Alzheimer tauopathies. *Ann Neurol.* 2017;81:117–128.

42. Ishiki A, Harada R, Kai H, et al. Neuroimaging-pathological correlations of [18F]THK5351 PET in progressive supranuclear palsy. *Acta Neuropathol Commun.* 2018;6:53.

43. Kroth H, Oden F, Molette J, et al. Discovery and preclinical characterization of [18F]PI-2620, a next-generation tau PET tracer for the assessment of tau pathology in Alzheimer's disease and other tauopathies. *Eur J Nucl Med Mol Imaging.* 2019;46:2178–2189.

44. Cho H, Choi JY, Hwang MS, et al. Subcortical 18F-AV-1451 binding patterns in progressive supranuclear palsy. *Mov Disord.* 2017;32:134–140.

45. Whitwell JL, Lowe VJ, Tosakulwong N, et al. [18F]AV-1451 tau positron emission tomography in progressive supranuclear palsy. *Mov Disord.* 2017;32:124–133.

46. Tagai K, Ono M, Kubota M, et al. High-contrast in vivo imaging of tau pathologies in Alzheimer's and non-Alzheimer's disease tauopathies. *Neuron.* 2021;109:42–58.e8.

47. Li L, Liu FT, Li M, et al.; Progressive Supranuclear Palsy Neuroimage Initiative (PSPNI). Clinical utility of 18F-APN-1607 tau PET imaging in patients with progressive supranuclear palsy. *Mov Disord.* 2021;36:2314–2323.

48. Whitwell JL, Tosakulwong N, Schwarz CG, et al. MRI outperforms [18F]AV-1451 PET as a longitudinal biomarker in progressive supranuclear palsy. *Mov Disord.* 2019;34:105–113.

49. Whitwell JL, Ahlskog JE, Tosakulwong N, et al. Pittsburgh compound B and AV-1451 positron emission tomography assessment of molecular pathologies of Alzheimer's disease in progressive supranuclear palsy. *Parkinsonism Relat Disord.* 2018;48:3–9.

50. Williams DR, Holton JL, Strand C, et al. Pathological tau burden and distribution distinguishes progressive supranuclear palsy-parkinsonism from Richardson's syndrome. *Brain.* 2007;130:1566–1576.